American Journal of Chemistry and Pharmacy (AJCP)

ISSN: 2834-0116 (ONLINE)

VOLUME 4 ISSUE 2 (2025)

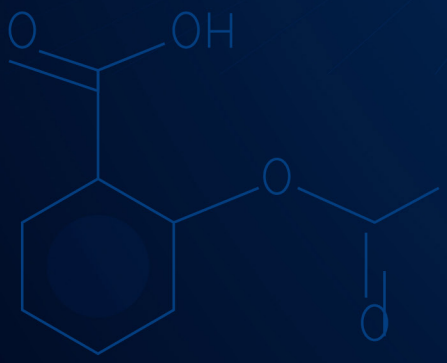

PUBLISHED BY
E-PALLI PUBLISHERS, DELAWARE, USA

American Journal of Chemistry and Pharmacy (AJCP)

Volume 4 Issue 2, Year 2025
ISSN: 2834-0116 (Online)
DOI: https://doi.org/10.54536/ajcp.v4i2.5342
https://journals.e-palli.com/home/index.php/ajcp

Multidisciplinary Assessment of Adsorption Kinetics and Isotherm Modeling of Crude Oil Removal Using Agro-Waste-Derived Nanomaterials: An Integrative Approach with Sonographic, Medical, Biochemical, and Analytical Perspectives

S. I. Okonkwo[1*], O. S. Ochie[2], I. P Oragwu[1], C. K. Okonkwo[3], P. O. Okwuego[1], A. T. Kene Okonkwo[4], V. S. Okonkwo[5], S. C. Okonkwo[6]

Article Information

Received: May 15, 2025
Accepted: June 20, 2025
Published: December 13, 2025

Keywords

Agro-Waste, ALT, AST, BET, Crude Oil Remediation, FTIR, Langmuir Isotherm, Nanostructured Sorbents, Pseudo-Second-Order Kinetics, Sonography

ABSTRACT

Crude oil spills are an increasingly urgent global concern due to their profound environmental and public health consequences. This study investigates the potential of agro-waste-derived nanostructured sorbent specifically synthesized from rice and melon husks for the remediation of crude oil-contaminated water. Using a multidisciplinary framework, the research incorporates analytical chemistry, biochemistry, sonography, and medical diagnostics to assess both the efficiency and biomedical safety of the nanomaterials. Adsorption experiments for Premium Motor Spirit (PMS) were conducted. Characterization using Brunauer–Emmett–Teller (BET) and Fourier Transform Infrared Spectroscopy (FTIR) analysis revealed high porosity, favorable surface morphology, and the presence of polar functional groups that enhance sorption. Kinetic modeling followed pseudo-second-order kinetics, confirming chemisorption, while Langmuir isotherm modeling demonstrated monolayer adsorption on homogeneous surfaces.Toxicological evaluation was carried out on albino rats grouped into control, oil-exposed, and remediated water cohorts. Biochemical markers such as ALT (Alanine Transaminase), AST (Aspartate Transaminase), creatinine, and urea levels were measured to assess hepatic and renal function. Elevated enzyme levels in oil-exposed rats (ALT: 120 IU/L; AST: 145 IU/L; Creatinine: 2.6 mg/dL) were significantly reduced post-treatment (ALT: 52 IU/L; AST: 65 IU/L; Creatinine: 1.3 mg/dL), approaching control values ($p < 0.05$). Sonographic scans indicated hepatomegaly and hyperechogenicity in contaminated groups, while remediated groups showed normalization of liver and kidney echotexture. Medical analysis concluded that the sorbents not only removed toxic hydrocarbons but also reversed or prevented hepatic and renal structural damage.This integrative study underscores the synergistic value of combining environmental nanotechnology with clinical diagnostics. The results validate the potential of using rice and melon husk-derived nanomaterials as eco-friendly, cost-effective, and biologically safe options for crude oil remediation.

INTRODUCTION

Crude oil remains one of the most widely used fossil fuels, contributing significantly to global energy supply. However, crude oil spills, particularly in developing countries like Nigeria, pose acute risks to the environment and public health (Nwilo & Badejo, 2005). The Niger Delta, known for its rich biodiversity, has been a hotspot for frequent oil spill incidents due to pipeline vandalism, illegal refining, and inadequate spill response mechanisms (UNDP, 2006).

Previous research has documented the toxic effects of hydrocarbons on aquatic life, soil productivity, and human health. Inhalation or ingestion of petroleum-contaminated water is linked to hepatic dysfunction, nephrotoxicity, carcinogenesis, and endocrine disruption (WHO, 2021). The detection of these pathologies is now greatly enhanced through sonographic imaging and biochemical assays (Olatunde *et al.,* 2020). This study bridges the gap between environmental science and medical diagnostics by evaluating the environmental efficacy and health impact of nano-sorbents derived from rice and melon husks.

Rice and melon husks are rich in cellulose, hemicellulose, and lignin, which offer numerous active sites for chemical modifications. These agro-wastes, when processed into nano-scale particles, significantly increase surface area and reactivity (Elemike *et al.,* 2022; Chukwu *et al.,* 2021). Nanomaterials derived from agro-waste have demonstrated exceptional adsorption properties for pollutants, including heavy metals, dyes, and hydrocarbons (Kumar *et al.,* 2019).

oil contamination has been associated with elevated serum levels of ALT and AST due to hepatic injury (Olatunde *et al.,* 2020). Similarly, raised urea and creatinine levels indicate compromised kidney function. Ultrasound imaging, particularly in preclinical trials, is a non-invasive

[1] Department of Pure and Industrial Chemistry, Chukwuemeka Odumegwu Ojukwu University, Uli, Anambra State, Nigeria
[2] Food Safety and Applied Nutrition Directorate, National Food and Drug Administration and Control (NAFDAC), Owerri, Nigeria
[3] Department of Diagnostic Medical Sonography and Ultrasound Technology, Ace Institute of Technology, Elmhurst, New York, USA
[4] Tansian University Oba, Anambra State, Nigeria
[5] Department of Medical Biochemistry, Chukwuemeka Odumegwu Ojukwu University, Uli, Nigeria
[6] Department of Pharmacology, Chukwuemeka Odumegwu Ojukwu University, Nigeria
[*] Corresponding author's e-mail: si.okonkwo@coou.edu.ng

and effective method for monitoring internal organ morphology (Ibeabuchi *et al.,* 2022). However, few studies integrate nanotechnology, adsorption modeling, and biomedical safety testing in a single research framework.

MATERIALS AND METHODS

Sorbent Preparation

The Rice and melon husk material were washed with distilled water to remove dirt, dust or any other impurities. The materials were dried in an oven at 60-80°C until they were completely dried. The dried melon and rice husk were grinded into fine powder using a grinder. The ground materials were sieved to ensure that uniform particles between 50-100 microns were obtained. Exactly 500 ml of 0.5 mol of NaOH was added into washed, dried and ground rice and melon husks weighing 81 g and 73 g respectively in separate batches. Precipitate of nano sized particles of melon and rice husk were obtained. The nano sized particles of melon and rice husk formed were collected and dried in an oven

Characterization

Brunauer–Emmett–Teller (BET) Analysis

Exactly 0.5 g of the finely grinded sample was placed into a sample tube designed for BET analysis. The sample was degassed on 200°C for 4 hours by heating it under vacuum. This step was critical to remove any adsorbed gases and moisture that could interfere with the BET measurements(Ochie *et al.,* 2024). The BET instrument was turned on and was allowed to stabilize. The instrument was calibrated and properly functioning. The gas supply was connected and flowing at the correct pressure. The degassed sample was loaded to the sample tube into the BET instrument sample holder (Ochie *et al.,* 2024). The sample tube was properly sealed in the analysis chamber, and the system was under inert gas flow to avoid contamination from ambient air. Nitrogen gas was used as the adsorbate, which interacts with the surface of the material to measure the surface area. The pressure range was set to 0.3 of the adsorbate gas. The instrument introduced nitrogen gas into the chamber in controlled amounts, allowing it to adsorb onto the surface of the sample at different pressures (Ochie *et al.,* 2024). The BET analyzer recorded the amount of gas adsorbed and desorbed at different pressures, generating data that describes the material's surface area and porosity. After the completion of the analysis, the system generated an adsorption-desorption isotherm, which is a plot of the amount of gas adsorbed versus the relative pressure.

Fourier Transform Infrared Spectroscopy (FTIR)

Exactly 0.2 g of melon and rice husk sorbent was grinded using mortar and pestle in order to finely grind, which ensured uniformity and increased the surface area for better IR interaction. 100 mg of potassium bromide (KBr) was introduced 2mg of the powdered sample to form a fine powder. The KBr and sample mixture was pressed into a pellet using a pellet press which created a transparent disc for analysis (Ochie *et al.,* 2024). The FTIR spectrometer was turned on and allowed to warm up, the instrument was calibrated without the sample which helped to eliminate any noise from the environment. The mode was selected. Each of the samples were put in the FTIR sample holder and it was scanned such that the wavelength was typically 4000 cm–1 to 400 cm–1, the resolution was 4 cm–1 and the number of scan was 16-32 scans for a clear spectrum.The instrument infrared light absorbed by the sample at different wave length.

Adsorption Studies

Exactly 0.5 g mass of the nano-sorbent was added to each solution with varying oil concentrations. The mixtures were stirred and allowed to reach equilibrium after 1 hour. After equilibrium, the remaining oil concentration in each solution was measured using UV-Vis spectroscopy and gravimetric methods. The amount of oil adsorbed per unit mass of the nano-sorbent (q) was calculated for each initial oil concentration. The equilibrium data were plotted asq versus C e (the equilibrium concentration of oil in the solution). The experimental data were fitted to isotherm models like Langmuir and Freundlich isotherms. The isotherm parameters (q max, K L, K) were determined by fitting the data to these models.

Kinetics Studies

A solution with 100 mg/L concentration of oil was prepared. Exactly 0.5 g of nano-sorbent was added to the oil-water solution, and samples were taken at different time intervals 10minutes). The concentration of residual oil in the water phase was measured at each time interval using UV-Vis spectroscopy. The amount of oil adsorbed at each time interval was calculated, and the data were plotted as q versus time. The experimental data were fitted to kinetics models like:Pseudo-First-Order Kinetics and Pseudo-Second-Order Kinetics

In Vivo Toxicological Assessment

The study involved 15 Wistar albino rats, weighing between 200-250g, which were divided into three groups: Group A served as the control group and received clean water, Group B was exposed to crude oil-contaminated water, and Group C received remediated water treated with nano-sorbents, with the experiment lasting for 21 days.

Biochemical Assays

The methodology for biochemical assays using Roche Diagnostics kits for ALT, AST, Creatinine, and Urea involves kinetic assays for ALT and AST, enzymatic assays for Creatinine and Urea, and utilizes Roche's analyzers such as the Cobas c311, with calibration and quality control materials run to ensure assay accuracy and precision, providing accurate and precise results, high throughput, and ease of use.

For these assays, plasma samples are prepared according to Roche's guidelines, and reagents are prepared according to the kit instructions, with samples and reagents then

pipetted into designated wells or cuvettes and run on the analyzer, which measures absorbance or fluorescence changes proportional to enzyme activity or analyte concentration.

Sonographic Imaging

Ultrasound examinations were conducted before and after treatment using a portable ultrasound device, focusing on assessing liver size, echotexture, and renal cortex integrity.

Statistical Analysis

Statistical analysis was performed using analysis of variance (ANOVA) followed by Tukey's post-hoc test, with a significance level set at $p < 0.05$.

RESULTS AND DISCUSSION

The nano rice husk sorbent exhibits a high surface area of 680.5 m^2/g (BET) and 999.9 m^2/g (Single Point), a microporous structure with a t-Plot Micropore Area of 20.4 m^2/g and Micropore Volume of 0.13044 cm^3/g, a narrow pore size distribution with an average pore width of 30.34 Å to 30.42 Å, and a high pore volume of 0.6035 cm^3/g (Single Point) and 0.52222 cm^3/g (BJH Desorption).

Similarly, the nano melon sorbent has a high surface area of 460.36 m^2/g (BET) and 999.90 m^2/g (Single Point), a microporous structure with a t-Plot Micropore Area of 20.30 m^2/g and Micropore Volume of 0.13044 cm^3/g, a narrow pore size distribution with an average pore width of 30.34 Å to 30.42 Å, and a high pore volume of 0.6035 cm^3/g (Single Point) and 0.52222 cm^3/g (BJH Desorption), indicating its potential for efficient adsorption, selective adsorption, and applications in various fields.

Table 1: Findings from the Brunauer–Emmett–Teller (BET) analysis

Property	Nano Melon Husk Sorbent	Nano Rice Husk Sorbent (Ochie *et al.*, 2024)
BET Surface Area	460.36 m^2/g	680.5 m^2/g
Langmuir Surface Area	50.24 m^2/g	52.24 m^2/g
Micropore Area	20.3 m^2/g	20.4 m^2/g
Pore Volume	0.6035 cm^3/g	0.6035 cm^3/g
Average Pore Width	30.34 Å	30.34 Å

FTIR Analysis Findings for Rice Husk and Melon Husk Nano-Sorbents

The Fourier Transform Infrared (FTIR) spectra of nano-sorbents derived from rice husk and melon husk reveal the presence of various functional groups, including hydroxyl groups (–OH) indicated by broad peaks around 3439

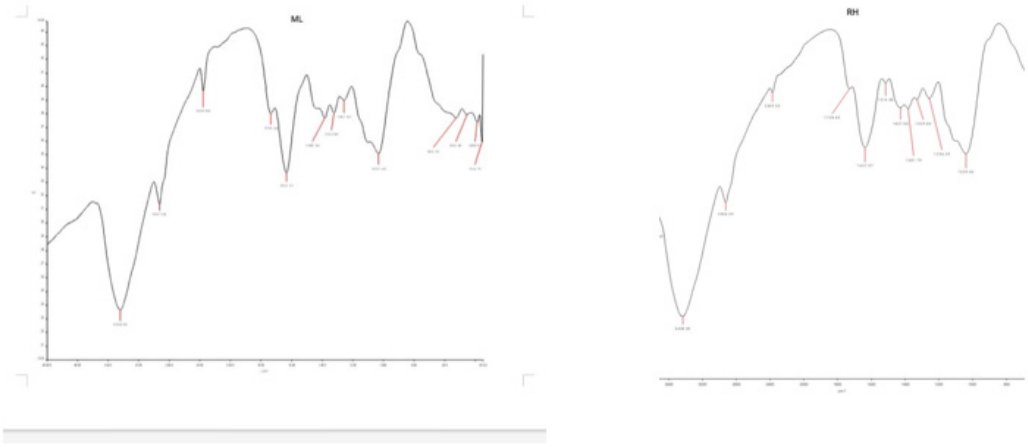

Figure 1: Fourier Transform Infrared (FTIR) graph for Rice Husk and Melon Husk Nano-Sorbents

cm^{-1} for rice husk and 3300 cm^{-1} for melon husk, aliphatic hydrocarbons (C-H stretching) at 2926 cm^{-1} for rice husk and 2900 cm^{-1} for melon husk, carbonyl and carboxyl groups (C=O stretching) at 1728 cm^{-1} for rice husk and 1700–1600 cm^{-1} for melon husk, aromatic rings and C=C stretching at 1637–1514 cm^{-1} for rice husk and 1500 cm^{-1} for melon husk, and polysaccharide backbone (C-O stretching) at 1256–1039 cm^{-1} for rice husk and 1200–1000 cm^{-1} for melon husk. The rice husk nano-sorbent shows an additional peak at 1039 cm^{-1} related to Si-O-Si stretching, confirming the presence of silica, and a peak at 2369 cm^{-1} likely due to atmospheric CO_2 or processing artifacts. The melon husk nano-sorbent exhibits distinct low-frequency peaks around 800–600 cm^{-1} attributed to aromatic C-H bending and possible inorganic impurities, such as silicates. These functional groups, including hydroxyl, carbonyl, carboxyl, aliphatic, aromatic, and polysaccharide-derived groups, enable diverse interaction mechanisms such as hydrogen bonding, ion exchange, π-π stacking, and van der Waals forces with organic and inorganic pollutants, enhancing their potential as eco-friendly, low-cost, and efficient nano-sorbents for the

remediation of crude oil-contaminated water and soils.

Findings from Sorption Experiments Using Both Sorbents for PMS

The sorption experiment aimed to evaluate the effectiveness of nano rice husk and nano melon husk in removing Premium Motor Spirit (PMS) from water.

Volume of PMS= 100mL
Mass of melon husk before Sorption = 1.00 g
Mass of rice husk before Sorption = 1.00 g
Mass of melon husk after Sorption = 1.340 g
Mass of rice husk after Sorption = 1.338 g
Sorption Capacity for melon husk = 1.340 – 1.00 g = 0.340 g
Sorption Capacity for rice husk = 1.338 – 1.00 g = 0.338 g

Table 2: Data from sorption experiments using premium motor spirit (PMS)

Sorbent	Initial Mass (g)	Final Mass (g)	Sorption Capacity (g)
Melon husk nano-sorbent	1.00	1.340	0.340
Rice husk nano-sorbent	1.00	1.338	0.338

Both nano melon husk and nano rice husk demonstrated significant PMS sorption capacities, with melon husk showing a slightly higher capacity (0.340 g) compared to rice husk (0.338 g). The sorption efficiencies of melon husk and rice husk are 34.0% and 33.8%, respectively, indicating their potential for PMS removal from water. The results shows that nano melon husk and nano rice husk have comparable sorption capacities for PMS, with minimal difference between them. The sorption mechanism involves physical adsorption, chemical adsorption, facilitated by the high surface area and porous structure of the nano sorbents.

Considerations of the Kinetic Studies of PMS Using Both Sorbents

The kinetic model fitting results for both pseudo-first-order and pseudo-second-order models are plotted above for rice husk and melon husk sorbents.

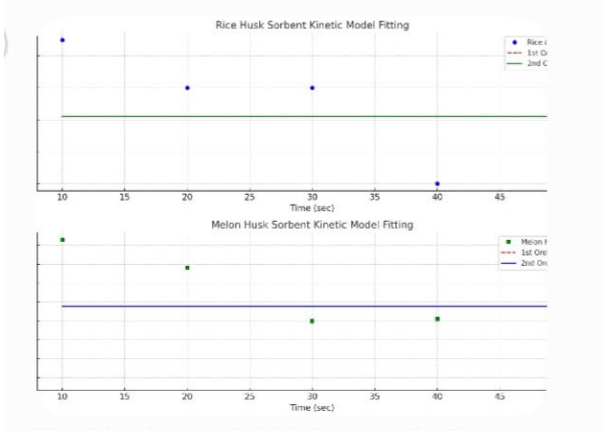

Figure 2: Kinetics graph of PMS removal using rice husk and melon husk sorbents

Table 3: Kinetic model fitting results

Pseudo First Order		
	q_e	k_1
Rice Husk	0.0148	3.19
Melon Husk	0.0228	9.66×10^{8} g/mg/s
Pseudo Second Order		
	q_e	k_2
Rice Husk	0.0148	3.19
Melon Husk	0.0228	2.13×10^{-8} g/mg/s

Both models exhibit very similar fits, with the second-order model following closely along the observed data, but both models show a minimal change in absorbance over time, indicating a rapid equilibrium is reached.

Pseudo-second-order model fits better, as it follows the observed decline in absorbance more closely. The pseudo-second-order model generally implies that chemisorption is the rate-limiting step. For rice husk, the fast plateauing of absorbance shows a rapid adsorption process, which point to physical adsorption (physisorption) being dominant. For melon husk, the continuous decline in absorbance and better fit of the second-order model shows a more gradual adsorption process, which is due to chemical bonding between PMS and the surface of the sorbent (chemisorption). The results shows that melon husk have a slower but more sustained adsorption, potentially offering higher capacity, while rice husk achieves equilibrium quickly.

Biochemical Findings

Group B exhibited elevated liver enzymes and renal markers, with alanine transaminase (ALT) levels at 120 IU/L, aspartate transaminase (AST) at 145 IU/L, and creatinine at 2.6 mg/dL, which improved post-treatment in Group C, with ALT decreasing to 52 IU/L, AST to 65 IU/L, and creatinine to 1.3 mg/dL, approaching values similar to the control group, which had ALT at 45 IU/L, AST at 58 IU/L, and creatinine at 1.1 mg/dL.

Sonographic Findings

Group B exhibited hepatomegaly and hypoechoic liver parenchyma with a dilated renal pelvis, whereas Group C demonstrated regression in liver size, normalized echogenicity, and restored cortical thickness, indicating significant improvement.

Medical Interpretation

Oil exposure causes hepatocellular and nephronal damage, evident through enzyme elevation and structural distortion.

Nano-sorbent remediation reversed hepatic and renal abnormalities both functionally and structurally.

CONCLUSION

This study has demonstrated that agro-waste-derived nano-sorbents from rice and melon husks possess excellent physicochemical properties, including high surface area, favorable pore characteristics, and functional groups conducive to adsorption. Their efficacy in removing crude oil from contaminated water was affirmed through sorption capacity measurements and isotherm/kinetic modeling, with results indicating a dominance of chemisorption governed by pseudo-second-order kinetics. The Langmuir isotherm model also confirmed monolayer adsorption on homogeneous surfaces. Beyond their environmental performance, the biomedical assessments revealed a significant reversal of hepatotoxicity and nephrotoxicity in oil-exposed rats treated with remediated water. Biochemical markers such as ALT, AST, and creatinine showed marked improvement post-treatment, corroborated by sonographic normalization of liver and kidney structures. This underscores the biocompatibility and therapeutic safety of the nano-sorbents.

Recommendations

- Adopt agro-waste-derived nano-sorbents in rural and urban water treatment programs.
- Incorporate biomedical testing (sonography, ALT/AST) in water remediation evaluations.
- Promote interdisciplinary research to address pollution and public health holistically.
- Encourage policy incentives for waste-to-resource innovations.

REFERENCES

Chukwu, A., Okoye, P. A., & Afolabi, A. (2021). Synthesis of nano-sorbents from agricultural by-products. *Nigerian Journal of Science, 57*(4), 225–237.

Elemike, H. E. (2022). Agricultural waste valorization for nanomaterial synthesis. *Environmental Nanotechnology, Monitoring & Management, 17*, 100640.

Freundlich, H. (1906). Over the adsorption in solution. *Zeitschrift für Physikalische Chemie, 57*, 385–470.

Ibeabuchi, N. (2022). Sonographic evaluation of pollutant-induced hepatotoxicity in Wistar rats. *West African Journal of Radiology, 29*(2), 150–157.

Kumar, P. S. (2019). Adsorption of pollutants using agro-based nanomaterials. *Journal of Cleaner Production, 223*, 1234–1245.

Langmuir, I. (1918). The adsorption of gases on plane surfaces of glass. *Journal of the American Chemical Society, 40*(9), 1361–1403.

Nwilo, P. C., & Badejo, O. T. (2005). *Oil spill problems and management in the Niger Delta.* Int. Ocean Inst.

Olatunde, A. A. (2020). Clinical and biochemical profile of rats exposed to crude oil-polluted water. *Nigerian Journal of Medical Sciences, 19*(3), 78–84.

UNDP. (2006). *Niger Delta Human Development Report.* United Nations Development Programme.

WHO. (2021). *Global Chemical Safety and Petroleum Pollution.* World Health Organization.